Observer-based event-triggered control for systems with slope-restricted nonlinearities

Luciano Moreira, Joao Gomes da Silva, Sophie Tarbouriech, Alexandre Seuret

Received: Added at production | Revised: Added at production | Accepted: Added at production

DOI: xxx/xxxx

RESEARCH ARTICLE

Observer-based event-triggered control for systems with slope-restricted nonlinearities

L. G. Moreira*[1] | J. M. Gomes da Silva Jr.[2] | S. Tarbouriech[3] | A. Seuret[3]

[1]DEPEX-CH, Instituto Federal de Educação, Ciência e Tecnologia Sul-rio-grandense (IFSul), Charqueadas-RS, Brazil
[2]PPGEE / DELAE, Universidade Federal do Rio Grande do Sul, Porto Alegre-RS, Brazil
[3] LAAS-CNRS, Université de Toulouse, CNRS, Toulouse, France

Correspondence
*Luciano Gonçalves Moreira, Email: lucianomoreira@charqueadas.ifsul.edu.br

Present Address
Rua General Balbão, 81. Charquadas - RS. Brazil. 96.745-000

Abstract

This paper presents an observer-based event-triggering strategy for systems with slope-restricted nonlinearities that depend on the state. Both the emulation and co-design problems are addressed. To avoid Zeno Behavior, a minimum dwell time is considered. By using a looped-functional approach and the cone-bounded properties of the nonlinearity, sufficient conditions based on linear matrix inequalities are derived to ensure global asymptotic stability of the origin of the closed-loop system under the proposed event-triggering strategy. These conditions are incorporated into convex optimization problems to optimally determine the event-triggering function parameters and the observer gain (in the co-design case) aiming at reducing the number of control updates. Numerical examples illustrate the potentialities of the approach.

KEYWORDS:
Event-triggered control, Nonlinear systems, Linear matrix inequalities, Aperiodic sampled-data control, Slope-restricted nonlinearities.

1 | INTRODUCTION

From a practical and technological point of view, event-triggered control strategies have been proposed as effective means to deal with communication and computation constraints in the context of networked control systems, i.e., systems where part or all of the communication is carried over a generic digital communication network (see [1,2,3,4] and the references therein). Moreover, in the case of wireless networks, reducing the transmissions also reduces energy consumption, which is important for remote battery-operated nodes.

In the event-triggered control paradigm, differently from the classical periodic sampled control case, transmission of data and updating of the control action takes place only when a triggering condition, usually based on the system state or output values, is violated. The design challenges are to compute the control law and the triggering condition aiming at reducing the number of events and consequently the number of plant input control updates while keeping the closed-loop system stable and/or satisfying some performance criteria. Moreover, due to the hybrid nature of the closed-loop system, it should also be guaranteed that no Zeno behavior occurs. A Zeno behavior is characterized by the occurrence of infinitely many events at the same instant or the occurrence of inter-event times that tend to zero as time goes to infinity or to a finite instant, i.e. accumulation points in the event instants sequence (see, for instance, [3,4] for an explanation of Zeno behavior).

Basically, two approaches for designing event-triggered controllers are found in the literature[4]. The first one is the so-called emulation design, where the controller is given *a priori* and the task is to design only the triggering condition. Among works

addressing emulation design, one can cite[4,5,6,7,8] in the context of linear systems while works[2,9,10,11] consider nonlinear systems. The second approach, referred in the literature as co-design, consists in designing the control law as well as the triggering condition simultaneously. It is addressed, for instance, in the papers[12,13,14,15] considering linear systems and in[16,17] considering nonlinear ones. Some recent works employ event-triggering techniques to tackle alternative problems as, for instance, multi-agent systems consensus[18], output regulation by means of adaptive controllers[19], output regulation and control by means of neural networks and self-learning techniques[20,21]. The approaches followed in these papers cannot be regarded neither as emulation nor as co-design.

Many works in the literature address event-triggered control assuming that the entire state information is available (e.g.[3,4,9,22,23,24,25,26]). Unfortunately, in most practical applications, only part of the system state or a measurable output is available and this represents an additional challenge for the design of the event-triggering rules since, in this context, it is harder to eliminate the possibility of Zeno behavior. In the context of limited information, the control system can be implemented considering output-based controllers or observer-based controllers. In the first case, an output-feedback controller and an event-triggering rule based only on the output information is designed. Among works using this approach we can cite Abdelrahim et al[10], which consider nonlinear systems and employ a hybrid system formalism[27] to derive LMI stability conditions alongside with dwell-time techniques to avoid Zeno behavior. Only emulation design is covered and the method needs *a priori* knowledge of a Lyapunov function for the closed-loop system. Still dealing with output-based feedback for nonlinear systems in an emulation design context, using dwell-time techniques and a hybrid systems formalism, Dolk et al[28] consider a dynamic triggering law, disturbances and network delays. The designer needs to find a hybrid system representation for the closed-loop system where the nonlinear terms are linearly-bounded with respect to the networked-induced error and also needs to know a Lyapunov function and a storage function that are suitable for the system. Passivity theory is employed by Yu and Antsaklis[29] to deal with input feed-forward output feedback passive (IF-OFP) nonlinear plants subject to communication delays and quantization. Only the emulation design case is addressed and their method needs the knowledge of a storage function with known passivity indexes. Absence of Zeno behavior is proved using the same arguments as in Tabuada's work[3]. More recently, Abdelrahim et al[8] considered the emulation design of output-based event-triggered controllers for linear systems with distributed sensors that feature signal amplitude quantization. The hybrid systems formalism is also employed in this work. The second option to deal with limited information is to incorporate a state observer and use the observed state in the feedback control law and in the evaluation of the event-triggering rule. In this context, Xia et al[30] derive LMI stability conditions for linear time invariant systems with norm-bound uncertainties. A relative error triggering criterion is considered. The control law and the observer gains must be given *a priori*, i.e. only the emulation design is addressed. On the other hand, Feng et al[31] address the co-design of all system elements (observer gains, controller gains and triggering rule parameters), considering periodic event-triggered control (PETC) and a specific class of nonlinear systems where the sum of the nonlinear components equals unity. This specific property is used to define a Lyapunov function and to derive LMI stability conditions that allow the co-design, as long as a set of constants are previously chosen by the designer. However, no method for choosing these constants is given and one needs to choose them by trial-and-error. Recently, Xing et al[32] addressed emulation design considering a specific class of nonlinear systems suitable for modeling, for instance, ship dynamics. To avoid Zeno behavior, a fixed threshold triggering strategy is employed and, therefore, only practical stability can be achieved, i.e. the resulting trajectories do not converge to the origin. In our previous work[33], linear systems subject to cone-bounded nonlinear inputs were addressed using observer-based techniques. The simultaneous synthesis of the controller gains and of the triggering rule parameters is obtained by numerically solving a convex optimization problem. A relative threshold triggering strategy is used to allow asymptotic stability and a minimum dwell time is introduced to avoid Zeno behavior. Exact discretization of the closed-loop system is employed to cope with the stability issues imposed by the minimum dwell time.

In the current paper, we address event-triggered controllers for systems with slope-restricted (as a consequence, sector-bounded) nonlinearities that depend on the state and are not measurable. Examples of practical nonlinearities that fit in this class include saturations, dead-zones, Chua's diodes[34], some trigonometric functions and generic continuous piecewise-linear nonlinearities, which can also be used to represent more generic functions satisfying sector bound conditions. The major contribution is to propose a design method based on convex optimization problems to compute the event-triggering function and as much as possible the controller and observer parameters. We consider the use of a nonlinear state observer to reconstruct the state from the available output information. This leads to the first challenge: since the nonlinearity value is not measurable and depends on the state, it is not possible to design an observer such that the nonlinearity cancels-out in the observation error dynamics, as can be done in the case of input nonlinearities[33]. This issue will be addressed by the introduction of an auxiliary nonlinear function that depends on the original nonlinearity and has some specific properties. Moreover, as the separation principle does not

hold in this case, conditions to certify the stability of the augmented closed-loop system are formally provided. Zeno behavior is avoided by imposing a dwell time[35] in the triggering condition. The introduction of the dwell time leads to the second challenge: coping with the stability issues imposed by the dwell time. Differently from[33], exact discretization cannot be applied here because the nonlinearity depends on the state value and thus it is not constant between events. To overcome this issue, a looped-functional approach[36,37,38] is considered to guarantee that the total variation of a quadratic Lyapunov function over the dwell time is strictly decreasing. Based on this approach and exploring the cone-bounded properties of the nonlinearities, conditions in the form of linear matrix inequalities (LMIs) are devised to ensure the global asymptotic stability of the origin under the proposed event-triggering strategy. These conditions are cast into convex optimization problems allowing to address the emulation design and a co-design case where the triggering condition and the observer gain matrix are computed at the same time. Differently from some aforementioned works on nonlinear systems, the Lyapunov function to certify the closed-loop stability and the parameters of the triggering function are simultaneously computed. Furthermore, as the conditions are given in an LMI form, an explicit optimization criterion on the triggering function parameters is proposed aiming at an effective reduction of the generated events, i.e. the reduction of the control updates. As a side effect of the conditions, the stability of the closed-loop nonlinear system under periodic sampled-data control, with period equal to the considered dwell time is also formally guaranteed.

The remaining of the paper is organized as follows. In Section 2, the system to be considered is described and the problem we intend to solve is formally stated. The proposed event-triggering strategy is introduced in Section 3. Section 4 presents some tools that will be instrumental to derive the main results of this work. In Sections 5 and 6, asymptotic stability conditions in the form of linear matrix inequalities are presented to address the problem in the emulation and in the co-design contexts, respectively. The convex optimization problems proposed as means of computing the triggering function and the observer parameters (in the co-design case) are presented in Section 7. Section 8 illustrates the potentialities of the proposed approach through two numerical examples. Section 9 draws some concluding remarks and directions of future works.

Notation. $\mathbb{N}$, $\mathbb{R}$, $\mathbb{R}^n$, $\mathbb{R}^{n\times m}$ denote respectively the sets of natural numbers, real numbers, n-dimensional real-valued vectors and $n \times m$ real-valued matrices. For a given positive scalar T, $\mathbb{F}^n_{[0,T]}$ denotes the set of differentiable functions from the interval $[0, T]$ into $\mathbb{R}^n$. For any matrix A, A' denotes its transpose. For any square matrix A, $\mathrm{tr}(A)$ denotes its trace and $\mathrm{He}(A) = A + A'$. For two symmetric matrices of the same dimensions, A and B, $A > B$ means that $A - B$ is symmetric positive definite. I and 0 stand respectively for the identity and the null matrix of appropriate dimensions. The block-diagonal matrix constructed from matrices X and Y is denoted by $\mathrm{diag}(X, Y)$. For a partitioned matrix, the symbol $*$ stands for symmetric blocks. $\lambda_{min}(A)$ and $\lambda_{max}(A)$ denote, respectively, the smallest and the largest eigenvalues of matrix A. $\|\cdot\|$ stands for the Euclidean norm.

2 | PROBLEM STATEMENT

Consider a continuous-time plant represented by the following equations:

$$\begin{cases} \dot{x}_p(t) = A_p x_p(t) + B_p u(t) + B_{pf} f(H x_p(t)) \\ y_p(t) = C_p x_p(t) \end{cases} \tag{1}$$

where $x_p(t) \in \mathbb{R}^n$, $u(t) \in \mathbb{R}^m$, $y_p(t) \in \mathbb{R}^p$ are the state, the input and the output of the plant, respectively. Matrices A_p, B_p, B_{pf}, C_p and H are constant and of appropriate dimensions. Function $f : \mathbb{R}^l \to \mathbb{R}^l$ is a slope-restricted, decentralized nonlinearity, i.e., each component $f_i : \mathbb{R} \to \mathbb{R}$, $i \in \{1, ..., l\}$ satisfies the following assumptions:

(A1) $f_i(0) = 0$.

(A2) $f_i(v_i)$ is continuous and differentiable by parts, satisfying

$$0 \leq \frac{df_i(v_i)}{dv_i} \leq \lambda_i;\ \lambda_i > 0,\ \forall v_i \in \mathbb{R}$$

Note that any system where the nonlinearities are cone-bounded and whose variation rate is upper-bounded fulfill assumptions (A1) and (A2). In particular, as it will be seen, a nonlinearity satisfying these assumptions will also verify a classical sector condition. As mentioned in the Introduction, examples of nonlinearities satisfying (A1) and (A2) include saturation, dead-zone, Chua's diodes[34], generic continuous piecewise-linear nonlinearities (which can be used to suitably approximate more complex nonlinearities), etc.

We consider the following observed-based feedback controller to asymptotically stabilize system (1):

$$\begin{cases} \dot{\hat{x}}(t) = A_p\hat{x}(t) + B_p u(t) + B_{pf} f(H\hat{x}(t)) - Le_y(t) \\ \hat{y}(t) = C_p\hat{x}(t) \\ u(t) = K\hat{x}(t) \end{cases} \tag{2}$$

where $\hat{x}(t) \in \mathbb{R}^n$ and $\hat{y}(t) \in \mathbb{R}^p$ are the state and the output of the observer, respectively, and $e_y(t) = y_p(t) - \hat{y}(t)$ is the output error. $L \in \mathbb{R}^{n\times p}$ and $K \in \mathbb{R}^{m\times n}$ are the observer and the observed state feedback gains, respectively.

Since our goal is to implement an event-triggered control strategy, the control action applied to the plant is supposed to be updated only at the instants t_k, $k \in \mathbb{N}$, determined by the event-triggering algorithm. We assume that $t_0 = 0$. The control action is held constant between two successive trigger events by means of a zero-order holder. Therefore, the actual control signal applied to the plant is given by:

$$u(t) = K\hat{x}(t_k), \qquad \forall t \in [t_k, t_{k+1}) \tag{3}$$

and the closed-loop system can be represented, $\forall t \in [t_k, t_{k+1})$, by:

$$\begin{cases} \dot{x}_p(t) = A_p x_p(t) + B_p u(t) + B_{pf} f(Hx_p(t)) \\ \dot{\hat{x}}(t) = A_p\hat{x}(t) + B_p u(t) + B_{pf} f(H\hat{x}(t)) - Le_y(t) \\ y_p(t) = C_p x_p(t) \\ \hat{y}(t) = C_p\hat{x}(t) \\ e_y(t) = y_p(t) - \hat{y}(t) \\ u(t) = K\hat{x}(t_k) \end{cases} \tag{4}$$

Define now the observation error $e(t) = x_p(t) - \hat{x}(t)$, the augmented state vector $x(t) = \left[\hat{x}'(t)\ e'(t)\right]' \in \mathbb{R}^{2n}$ and the vector of available information to the event generator $y_a(t) = \left[\hat{x}'(t)\ e_y'(t)\right]' \in \mathbb{R}^{n+p}$ and the following auxiliary nonlinearity:

$$\begin{aligned} \rho(e, \hat{x}) &= f(Hx_p) - f(H\hat{x}) \\ &= f(H\hat{x} + He) - f(H\hat{x}) \end{aligned}$$

The closed-loop system can therefore be represented, $\forall t \in [t_k, t_{k+1})$, $\forall k \in \mathbb{N}$, as follows:

$$\begin{cases} \dot{x}(t) = A_a x(t) + B_a u(t) + B_{af} f(H_1 x(t)) + B_{a\rho}\rho(H_2 x(t), H_1 x(t)) \\ u(t) = \begin{bmatrix} K & 0 \end{bmatrix} x(t_k) \\ y_a(t) = C_a x(t) \end{cases} \tag{5}$$

with

$$\begin{gathered} A_a = \begin{bmatrix} A_p & -LC_p \\ 0 & A_p + LC_p \end{bmatrix},\ B_a = \begin{bmatrix} B_p \\ 0 \end{bmatrix},\ C_a = \begin{bmatrix} I & 0 \\ 0 & C_p \end{bmatrix},\ B_{af} = \begin{bmatrix} B_{pf} \\ 0 \end{bmatrix},\ B_{a\rho} = \begin{bmatrix} 0 \\ B_{pf} \end{bmatrix}, \\ H_1 = \begin{bmatrix} H & 0 \end{bmatrix},\ H_2 = \begin{bmatrix} 0 & H \end{bmatrix}, \\ \rho(H_2 x(t), H_1 x(t)) = f(H_1 x(t) + H_2 x(t)) - f(H_1 x(t)). \end{gathered} \tag{6}$$

Remark 1. We are assuming that the value of the nonlinearity $f(Hx_p(t))$ is not measurable. The observer dynamics consider therefore a term $f(H\hat{x}(t))$. In this case, the plant nonlinearity is not canceled in the observer error dynamics. Indeed, this dynamics depends on the difference between the values of $f(Hx_p(t))$ and $f(H\hat{x}(t))$, which is given by the auxiliary nonlinearity $\rho(e, \hat{x}) = \rho(H_1 x(t), H_2 x(t))$. This fact leads to a more involved stabilization problem, since the separation principle is not valid in this case and we have to deal with two nonlinearities in the loop: f and ρ. Addressing this issue constitutes one novelty introduced in the present paper. Note that in the particular case in which $f(Hx_p(t))$ is considered measurable, this term can be considered in the observer (instead of $f(H\hat{x}(t))$) and the error dynamics become linear. This would be similar to the case of input nonlinearities addressed in [33] or to the approach considered in [39] to design output feedback controllers for Lur'e type systems.

Considering system (5), the following problems are addressed in this work:

Problem 1 (*Emulation design*)**.** Assuming that an observer and a stabilizing state feedback have been designed to ensure the global asymptotic stability of the continuous closed-loop system formed by the direct connection between (1) and (2), design an event-triggered control algorithm in order to guarantee the global asymptotic stability of the origin of the closed-loop system (5), while implicitly reducing the control updates (i.e. the number of events).

Problem 2 (*Observer co-design*)**.** Assuming that only a stabilizing state feedback is given, jointly design the event-triggered control algorithm and the observer gain to ensure the global asymptotic stability of the origin of the closed-loop system.

3 | EVENT-TRIGGERING STRATEGY

The triggering rule defines the instants t_k when events are generated and the value of the control signal is updated. To be able to obtain asymptotic stability, a relative threshold triggering strategy is considered. Differently from the fixed threshold triggering strategy employed in[32], which allows to avoid Zeno behavior at the expense of attaining only practical stability, here we employ a time regularization (introduction of a minimum dwell time[35] T) to deal with this issue.

Defining the error between the value of the observer state at the last triggering instant and at the current time as

$$\delta(t) = \hat{x}(t_k) - \hat{x}(t) \tag{7}$$

the considered triggering rule is then given by:

$$t_{k+1} = \min\{t \geq t_k + T, \quad s.t. \quad g(\delta(t), y_a(t)) \geq 0\}, \tag{8}$$

where $g(\delta(t), y_a(t))$ is defined as follows:

$$g(\delta(t), y_a(t)) = \delta(t)' Q_\delta \delta(t) - y_a'(t) Q_\epsilon^{-1} y_a(t), \tag{9}$$

with Q_δ and Q_ϵ being positive-definite matrices of appropriate dimensions.

It should be noticed that the triggering function $g(\delta(t), y_a(t))$ in (9), which is also used in our previous work[33], can be seen as a generalization of the one introduced in[3]. Here the relative error components are weighted by the positive definite matrices Q_δ and Q_ϵ, leading to more degrees of freedom and potentially less events generation.

The parameters Q_δ and Q_ϵ of the function $g : \mathbb{R}^n \times \mathbb{R}^{n+p} \to \mathbb{R}$ and the minimum dwell time $T > 0$ have to be designed such that the asymptotic stability of the origin of system (5) is ensured when the event instants t_k are determined by (8). Since $\delta(t)$ depends only on the observed state $\hat{x}(t)$, on its sampled value at t_k and on $y_a(t) = \begin{bmatrix} \hat{x}'(t) & e_y'(t) \end{bmatrix}'$, the triggering rule needs only available information (i.e. the plant output and the observer state). Notice that, after each event, the controller is forced to wait at least T units of time before evaluating function g again. Thus, rule (8) ensures a minimum inter-event time equal to the minimum dwell time T and no Zeno behavior can occur.

The stability analysis should therefore be split into two intervals: $[t_k, t_k + T)$ and $[t_k + T, t_{k+1})$. From a Lyapunov perspective, the basic idea consists in considering a Lyapunov candidate function V that verifies the following conditions for all $k \in \mathbb{N}$:

(i) $V(x(t_k + T)) < V(x(t_k))$

(ii) $\dot{V}(x(t)) < 0, \quad \forall t \in [t_k + T, t_{k+1})$.

This approach has been applied in[33]. However, in that case, as the nonlinearity was on the input, an exact discretization of the system considering a period T was possible and (i) reduced to a discrete-time test of stability. In the present problem, as the nonlinearity affects the state, exact discretization is not possible. Thus, in order to ensure (i), considering that the control signal is kept constant during the interval $[t_k, t_k + T)$, we propose in the present work an approach based on the use of a looped-functional, which has been successfully applied to the stability analysis of sampled-data linear systems[37]. It should be emphasized that condition (i) does not imply that $V(x(t))$ is strictly decreasing in the interval $(t_k, t_k + T)$, i.e. $\dot{V}(x(t))$ is not required to be negative during this interval.

4 | INSTRUMENTAL TOOLS

In this section we provide two instrumental lemmas to tackle the nonlinearities f and ρ in the stability conditions. The first one is a classical sector condition that is satisfied by the system nonlinearity f.

Lemma 1. If each component of f satisfies the assumptions (A1) - (A2), then

$$f'(v) S_f (f(v) - \Lambda v) \leq 0 \tag{10}$$

where $\Lambda = \text{diag}(\lambda_1, ..., \lambda_l)$ and S_f is any diagonal positive-definite $l \times l$ matrix, is satisfied $\forall v \in \mathbb{R}^l$.

Proof. Consider each component f_i of f and its corresponding argument, v_i. If $v_i \geq 0$, application of the Mean Value Theorem and the assumptions imply $f_i(v_i) \geq f_i(0) = 0$ and $f_i(v_i) \leq \lambda_i v_i$. If $v_i < 0$, similar arguments lead to $f_i(v_i) \leq f_i(0) = 0$ and $f_i(v_i) \geq \lambda_i v_i$. Therefore, $f_i(v_i)\sigma_i(f_i(v_i) - \lambda_i v_i) \leq 0$, $\forall v_i \in \mathbb{R}$, $\forall \sigma_i > 0$. Since f is decentralized, relation (10) directly follows with $S_f = \text{diag}(\sigma_1, ..., \sigma_l)$. □

To handle the nonlinearity $\rho(H_2x(t), H_1x(t)) = f(H_1x(t)+H_2x(t))-f(H_1x(t))$, defined in (6), the following result is stated.

Lemma 2. Consider the nonlinearity $\rho(v_1, v_0) = f(v_0 + v_1) - f(v_0)$ as defined in (6). If each component of f satisfies the assumptions (A1) - (A2), then

$$\rho'(v_1, v_0)S_\rho(\rho(v_1, v_0) - \Lambda v_1) \leq 0 \tag{11}$$

where $\Lambda = \text{diag}(\lambda_1, ..., \lambda_l)$ and S_ρ is any diagonal positive-definite $l \times l$ matrix, is satisfied $\forall v_1, v_0 \in \mathbb{R}^l$.

Proof. Consider each component ρ_i of ρ and its corresponding arguments v_{1i} and v_{0i}, which are scalars.

If $v_{1i} \geq 0$, the assumptions on the lower-bound of the derivative of f_i imply that f_i is monotonically increasing, i.e., $f_i(v_{0i} + v_{1i}) \geq f_i(v_{0i})$, or, equivalently, $f_i(v_{0i} + v_{1i}) - f_i(v_{0i}) \geq 0$, leading to $\rho_i(v_{1i}, v_{0i}) \geq 0$. The upper-limit of the derivative leads, by applying the Mean Value Theorem, to $f_i(v_{0i} + v_{1i}) - f_i(v_{0i}) \leq \lambda_i v_{1i}$, i.e. $\rho_i(v_{1i}, v_{0i}) - \lambda_i v_{1i} \leq 0$.

If $v_{1i} < 0$, a similar analysis brings $\rho_i(v_{1i}, v_{0i}) \leq 0$ and $\rho_i(v_{1i}, v_{0i}) - \lambda_i v_{1i} \geq 0$.

Hence, $\rho_i(v_{1i}, v_{0i})\sigma_i(\rho_i(v_{1i}, v_{0i}) - \lambda_i v_{1i}) \leq 0, \forall \sigma_i > 0$ and relation (11) directly follows with $S_\rho = \text{diag}(\sigma_1, ..., \sigma_l)$.

□

5 | EMULATION DESIGN

In this section, the emulation case is addressed. Considering a given dwell time T, the goal is to propose a way to design the parameters Q_δ and Q_ϵ of the triggering function given in (9) assuming the controller and observer gains, K and L respectively, have been computed *a priori* in order to ensure that the origin of the continuous-time system (1)-(2) is globally asymptotically stable. In such a case, the following theorem establishes conditions for the global asymptotic stability of the closed-loop system origin under the event-triggering strategy.

Theorem 1. Considering T, K and L given, if there exist symmetric positive definite matrices Q_δ, Q_ϵ, P and R, a symmetric matrix F_1, matrices $Y_1, Y_2, Y_{1c}, Y_{2c}, F_2, N$ and X and positive definite diagonal matrices S_f, S_ρ, S_{fc} and $S_{\rho c}$ satisfying the LMIs

$$\Pi_1 + T(\Pi_2 + \Pi_3) < 0 \tag{12}$$

$$\begin{bmatrix} \Pi_1 - T\Pi_3 & TN \\ * & -TR \end{bmatrix} < 0 \tag{13}$$

$$\begin{bmatrix} \Pi_a & \Pi_b' \\ * & -Q_\epsilon \end{bmatrix} < 0 \tag{14}$$

with [1]

$$\begin{aligned}
\Pi_1 &= \text{He}\left\{M_1'PM_3 - NM_{12} - M_{12}'F_2M_2 + (M_1'Y_1' + M_3'Y_2')\left[A_aM_1 + B_a\left[K\ 0\right]M_2 - M_3 + B_{af}M_4 + B_{a\rho}M_5\right]\right. \\
&\quad \left. -M_4'S_f(M_4 - \Lambda H_1M_1) - M_5'S_\rho(M_5 + \Lambda H_2M_1)\right\} - M_{12}'F_1M_{12}, \\
\Pi_2 &= \text{He}\{M_3'(F_1M_{12} + F_2M_2)\} + M_3'RM_3, \\
\Pi_3 &= M_2'XM_2, \\
\Pi_a &= \text{He}\left\{M_1'PM_2 - M_4'S_{fc}(M_4 - \Lambda H_1M_1) - M_5'S_{\rho c}(M_5 - \Lambda H_2M_1)\right. \\
&\quad \left. +(M_1'Y_{1c}' + M_2'Y_{2c}')\left[(A_a + B_a\left[K\ 0\right])M_1 - M_2 + B_aKM_3 + B_{af}M_4 + B_{a\rho}M_5\right]\right\} - M_3'Q_\delta M_3, \\
\Pi_b &= C_aM_1,
\end{aligned}$$

$$\begin{aligned}
M_1 &= \left[I\ 0\ 0\ 0\ 0\right], \quad M_2 = \left[0\ I\ 0\ 0\ 0\right], \quad M_3 = \left[0\ 0\ I\ 0\ 0\right], \\
M_4 &= \left[0\ 0\ 0\ I\ 0\right], \quad M_5 = \left[0\ 0\ 0\ 0\ I\right], \quad M_{12} = M_1 - M_2,
\end{aligned} \tag{15}$$

then the origin of system (5) with the triggering rule defined by (8) and (9) is globally asymptotically stable.

[1] Notice that the selector matrices M_i in (12) and (13) differ from those in (14) in the dimensions of the third element.

Proof. Consider a quadratic function $V(x(t)) = x(t)'Px(t)$. The stability analysis is carried out considering two intervals, namely $[t_k, t_k + T)$ and $[t_k + T, t_{k+1})$. The first interval corresponds to the dwell time, in which the triggering function is not evaluated. We are going to show that conditions (12)-(14) ensure $V(x(t_k+T))-V(x(t_k)) < 0$, $\forall k \in \mathbb{N}$ and $\dot{V}(x(t)) < 0$, $\forall t \in [t_k+T, t_{k+1})$, $\forall k \in \mathbb{N}$.

For $t \in [t_k, t_k + T)$, we represent the system trajectories in a lifted domain[37,40,38] by defining $\tau = t - t_k$, with $\tau \in [0, T)$, and a function $\mathcal{X}_k(\tau) = x(t_k + \tau) = x(t)$, leading from (5) to the following equation:

$$\dot{\mathcal{X}}_k(\tau) = A_a\mathcal{X}_k(\tau) + B_a\begin{bmatrix}K & 0\end{bmatrix}\mathcal{X}_k(0) + B_{af}f(H_1\mathcal{X}_k(\tau)) + B_{a\rho}\rho(H_2\mathcal{X}_k(\tau), H_1\mathcal{X}_k(\tau)), \quad \forall\tau \in [0, T). \tag{16}$$

Moreover, for $t \in [t_k, t_k + T)$, we have:

$$V(x(t)) = V(\mathcal{X}_k(\tau)) = \mathcal{X}_k'(\tau)P\mathcal{X}_k(\tau), \quad \tau \in [0, T). \tag{17}$$

Consider now the solution to (16) for $\tau \in [0, T]$ given by $\mathcal{X}_k \in \mathbb{F}^{2n}_{[0,T]}$ and define:

$$W(\tau, \mathcal{X}_k) = V(\mathcal{X}_k(\tau)) + V_0(\tau, \mathcal{X}_k), \tag{18}$$

with $V_0(\tau, \mathcal{X}_k) : [0, T] \to \mathbb{F}^{2n}_{[0,T]}$ being a looped-functional borrowed from[36,37], defined as follows:

$$\begin{aligned} V_0(\tau, \mathcal{X}_k) = {} & (T - \tau)(\mathcal{X}_k(\tau) - \mathcal{X}_k(0))'\left[F_1(\mathcal{X}_k(\tau) - \mathcal{X}_k(0)) + 2F_2\mathcal{X}_k(0)\right] \\ & + (T - \tau)\tau\mathcal{X}_k'(0)X\mathcal{X}_k(0) + (T - \tau)\int_0^\tau \dot{\mathcal{X}}_k'(\theta)R\dot{\mathcal{X}}_k(\theta)d\theta. \end{aligned} \tag{19}$$

Observe that V_0 verifies a looping condition; i.e. $V_0(T, \mathcal{X}_k) = V_0(0, \mathcal{X}_k) = 0$, $\forall\mathcal{X}_k \in \mathbb{F}^{2n}_{[0,T]}$. Besides that, we have:

$$\begin{aligned} \dot{W}(\tau, \mathcal{X}_k) = {} & 2\mathcal{X}_k'(\tau)P\dot{\mathcal{X}}_k(\tau) + (T - \tau)\dot{\mathcal{X}}_k'(\tau)\left[R\dot{\mathcal{X}}_k(\tau) + 2F_1(\mathcal{X}_k(\tau) - \mathcal{X}_k(0)) + 2F_2\mathcal{X}_k(0)\right] \\ & - (\mathcal{X}_k(\tau) - \mathcal{X}_k(0))'\left[F_1(\mathcal{X}_k(\tau) - \mathcal{X}_k(0)) + 2F_2\mathcal{X}_k(0)\right] + (T - 2\tau)\mathcal{X}_k'(0)X\mathcal{X}_k(0) - \int_0^\tau \dot{\mathcal{X}}_k'(\theta)R\dot{\mathcal{X}}_k(\theta)d\theta. \end{aligned} \tag{20}$$

We show now that (12) and (13) imply $\dot{W}(\tau, \mathcal{X}_k) < 0$. With this aim, consider the following augmented vector:

$$\xi_k(\tau) = \left[\mathcal{X}_k'(\tau)\ \ \mathcal{X}_k'(0)\ \ \dot{\mathcal{X}}_k'(\tau)\ \ f'(\tau)\ \ \rho'(\tau)\right]' \tag{21}$$

where we are using the shortcuts $f(\tau) = f(H_1\mathcal{X}_k(\tau))$ and $\rho(\tau) = \rho(H_2\mathcal{X}_k(\tau), H_1\mathcal{X}_k(\tau))$ for simplicity.

The coupling relation between the components of $\xi_k(\tau)$ imposed by (16) leads to the following relation, valid for any matrices Y_1 and Y_2 of appropriate dimensions:

$$2\left(\mathcal{X}'(\tau)Y_1' + \dot{\mathcal{X}}_k'(\tau)Y_2'\right)M_0\xi_k(\tau) = 0, \tag{22}$$

with $M_0 = \begin{bmatrix}A_a & B_a\begin{bmatrix}K & 0\end{bmatrix} & -I & B_{af} & B_{a\rho}\end{bmatrix}$. Therefore, this null term can be added to the inequality (20). Combining (20) and (22) leads to

$$\begin{aligned} \dot{W}(\tau, \mathcal{X}_k) = {} & 2\mathcal{X}_k'(\tau)P\dot{\mathcal{X}}_k(\tau) + (T - \tau)\dot{\mathcal{X}}_k'(\tau)\left[R\dot{\mathcal{X}}_k(\tau) + 2F_1(\mathcal{X}_k(\tau) - \mathcal{X}_k(0)) + 2F_2\mathcal{X}_k(0)\right] \\ & - (\mathcal{X}_k(\tau) - \mathcal{X}_k(0))'\left[F_1(\mathcal{X}_k(\tau) - \mathcal{X}_k(0)) + 2F_2\mathcal{X}_k(0)\right] + (T - 2\tau)\mathcal{X}_k'(0)X\mathcal{X}_k(0) \\ & - \int_0^\tau \dot{\mathcal{X}}_k'(\theta)R\dot{\mathcal{X}}_k(\theta)d\theta + 2(\mathcal{X}'(\tau)Y_1' + \dot{\mathcal{X}}_k'(\tau)Y_2')M_0\xi_k(\tau). \end{aligned} \tag{23}$$

Now taking into account that for any matrix N of appropriate dimensions the following inequality is verified[37,41]

$$\int_0^\tau \dot{\mathcal{X}}_k'(\theta)R\dot{\mathcal{X}}_k(\theta)d\theta \geq 2\xi_k'(\tau)N(\mathcal{X}_k(\tau) - \mathcal{X}_k(0)) - \tau\xi_k'(\tau)NR^{-1}N'\xi_k(\tau), \tag{24}$$

one obtains that

$$\begin{aligned} \dot{W}(\tau, \mathcal{X}_k) \leq {} & 2\mathcal{X}_k'(\tau)P\dot{\mathcal{X}}_k(\tau) + (T - \tau)\dot{\mathcal{X}}_k'(\tau)\left[R\dot{\mathcal{X}}_k(\tau) + 2F_1(\mathcal{X}_k(\tau) - \mathcal{X}_k(0)) + 2F_2\mathcal{X}_k(0)\right] \\ & - (\mathcal{X}_k(\tau) - \mathcal{X}_k(0))'\left[F_1(\mathcal{X}_k(\tau) - \mathcal{X}_k(0)) + 2F_2\mathcal{X}_k(0)\right] + (T - 2\tau)\mathcal{X}_k'(0)X\mathcal{X}_k(0) \\ & - 2\xi_k'(\tau)N(\mathcal{X}_k(\tau) - \mathcal{X}_k(0)) + \tau\xi_k'(\tau)NR^{-1}N'\xi_k(\tau) + 2(\mathcal{X}'(\tau)Y_1' + \dot{\mathcal{X}}_k'(\tau)Y_2')M_0\xi_k(\tau). \end{aligned} \tag{25}$$

Moreover, considering that Lemma 1 and Lemma 2 ensure $f'(\tau)S_f(f'(\tau)-\Lambda H_1\mathcal{X}_k(\tau)) \leq 0$ and $\rho'(\tau)S_\rho(\rho(\tau)-\Lambda H_2\mathcal{X}_k(\tau)) \leq 0$, one obtains that

$$\begin{aligned}\dot{W}(\tau,\mathcal{X}_k) \leq\ & 2\mathcal{X}_k'(\tau)P\dot{\mathcal{X}}_k(\tau) + (T-\tau)\dot{\mathcal{X}}_k'(\tau)\left[R\dot{\mathcal{X}}_k(\tau) + 2F_1(\mathcal{X}_k(\tau)-\mathcal{X}_k(0)) + 2F_2\mathcal{X}_k(0)\right] \\ & - (\mathcal{X}_k(\tau)-\mathcal{X}_k(0))'\left[F_1(\mathcal{X}_k(\tau)-\mathcal{X}_k(0)) + 2F_2\mathcal{X}_k(0)\right] + (T-2\tau)\mathcal{X}_k'(0)X\mathcal{X}_k(0) \\ & - 2\xi_k'(\tau)N(\mathcal{X}_k(\tau)-\mathcal{X}_k(0)) + \tau\xi_k'(\tau)NR^{-1}N'\xi_k(\tau) + 2(\mathcal{X}'(\tau)Y_1' + \dot{\mathcal{X}}_k'(\tau)Y_2')M_0\xi_k(\tau) \\ & - f'(\tau)S_f(f'(\tau)-\Lambda H_1\mathcal{X}_k(\tau)) - \rho'(\tau)S_\rho(\rho(\tau)-\Lambda H_2\mathcal{X}_k(\tau)).\end{aligned} \tag{26}$$

Performing some algebraic manipulations, (26) can be rewritten as

$$\dot{W}(\tau,\mathcal{X}_k) \leq \xi_k'(\tau)\left[\Pi_1 + (T-\tau)\Pi_2 + (T-2\tau)\Pi_3 + \tau NR^{-1}N'\right]\xi_k(\tau). \tag{27}$$

Now, notice that the matrix expression in the right-hand side of (27) is affine with respect to τ. Thus, as $\tau \in [0,T]$, by convexity, it suffices to ensure that the right-hand-side of (27) is negative for $\tau = 0$ and for $\tau = T$ to guarantee that $\dot{W}(\tau,\mathcal{X}_k) < 0$, $\forall\tau \in [0,T]$. Applying the values $\tau = 0$ and $\tau = T$ to (27) leads to the following conditions:

$$\Pi_1 + T(\Pi_2 + \Pi_3) < 0, \tag{28}$$

$$\Pi_1 - T\Pi_3 + TNR^{-1}N' < 0. \tag{29}$$

Applying now the Schur complement to (29), one retrieves condition (13) and concludes that satisfaction of conditions (12) and (13) ensures $\dot{W}(\tau,\mathcal{X}_k) < 0$, $\forall\tau \in [0,T]$. This, in turn, ensures that

$$\int_0^T \dot{W}(\tau,\mathcal{X}_k)d\tau = V(\mathcal{X}_k(T)) - V(\mathcal{X}_k(0)) + V_0(T,\mathcal{X}_k) - V_0(0,\mathcal{X}_k) < 0. \tag{30}$$

Since $V_0(T,\mathcal{X}_k) = V_0(0,\mathcal{X}_k) = 0$, we conclude that satisfaction of conditions (12) and (13) ensures that

$$V(\mathcal{X}_k(T)) - V(\mathcal{X}_k(0)) = V(x(t_k+T)) - V(x(t_k)) < 0,\ \forall k \in \mathbb{N}. \tag{31}$$

For $t \in [t_k+T, t_{k+1})$, we can consider the signal $\delta(t)$, defined in (7) to re-write system (5) as follows:

$$\dot{x}(t) = \left(A_a + B_a\begin{bmatrix}K & 0\end{bmatrix}\right)x(t) + B_aK\delta(t) + B_{af}f\left(H_1x(t)\right) + B_{a\rho}\rho\left(H_2x(t), H_1x(t)\right) \tag{32}$$

Now, consider the following expression where $\dot{V}(x)$ is combined with the negative terms $f'(\tau)S_{fc}(f(\tau) - \Lambda H_1\mathcal{X}_k(\tau))$, $\rho'(\tau)S_{\rho c}(\rho(\tau) - \Lambda H_2\mathcal{X}_k(\tau))$ and $g(\delta(t), y_a(t))$:

$$\mathcal{L}_c = \dot{V}(x) - g(\delta(t), y_a(t)) - 2f'(t)S_{fc}(f(t) - \Lambda H_1x(t)) - 2\rho'(t)S_{\rho c}(\rho(t) + \Lambda H_2x(t)) \tag{33}$$

If we ensure $\mathcal{L}_c < 0$, since relations (10) and (11) hold, and relation $g(\delta(t), y_a(t)) \leq 0$ is ensured by the triggering condition (8) for any $t \in [t_k+T, t_{k+1})$, then it follows that $\dot{V}(x) < g(\delta(t), y_a(t)) - 2f'(t)S_{fc}(f(t)-\Lambda H_1x(t)) - 2\rho'(t)S_{\rho c}(\rho(t)+\Lambda H_2x(t)) \leq 0$ for any $t \in [t_k+T, t_{k+1})$.

Defining the vector

$$\xi(t) = \begin{bmatrix}x'(t) & \dot{x}'(t) & \delta'(t) & f'(t) & \rho'(t)\end{bmatrix}' \tag{34}$$

where the shortcuts $f(t) = f(H_1x(t))$ and $\rho(t) = \rho(H_2x(t), H_1x(t))$ are used for simplicity, we can rewrite (33) as:

$$\mathcal{L}_c = \xi'(t)\{\mathrm{He}\{M_1'PM_2 - M_3'Q_\delta M_3 + M_1'C_a'Q_\epsilon^{-1}C_aM_1 - M_4'S_{fc}(M_4 - \Lambda H_1M_1) - M_5'S_{\rho c}(M_5 + \Lambda H_2M_1)\}\}\xi(t). \tag{35}$$

Using the coupling between the components of ξ imposed by (32), the following relation is satisfied for any matrices Y_{1c} and Y_{2c} of appropriate dimensions:

$$2\left(x'(t)Y_{1c}' + \dot{x}'(t)Y_{2c}'\right)M_{0c}\xi(t) = 0 \tag{36}$$

with $M_{0c} = \begin{bmatrix}A_a + B_a\begin{bmatrix}K & 0\end{bmatrix} & -I & B_aK & B_{af} & B_{a\rho}\end{bmatrix}$. Hence, the left-hand side of (36) can be added to $\mathcal{L}_c$ without changing its value, leading to:

$$\begin{aligned}\mathcal{L}_c &= \xi'(t)\left\{\mathrm{He}\left\{M_1'PM_2 - M_3'Q_\delta M_3 + M_1'C_a'Q_\epsilon^{-1}C_aM_1 - M_4'S_{fc}(M_4 - \Lambda H_1M_1)\right.\right. \\ &\quad \left.\left. - M_5'S_{\rho c}(M_5 + \Lambda H_2M_1) + (M_1'Y_{1c}' + M_2'Y_{2c}')M_{0c}\right\}\right\}\xi(t) \\ &= \xi'(t)\left(\Pi_a + \Pi_b'Q_\epsilon^{-1}\Pi_b\right)\xi(t).\end{aligned} \tag{37}$$

Therefore, satisfying $\Pi_a + \Pi_b'Q_\epsilon^{-1}\Pi_b < 0$ ensures $\mathcal{L}_c < 0$ and thus $\dot{V}(x) < 0$, $\forall t \in [t_k+T, t_{k+1})$ when $g(\delta(t), y_a(t))$ is given as in (9). Applying the Schur complement to this last inequality we recover (14). Hence, satisfaction of (14) effectively ensures that $\dot{V}(x) < 0$, $\forall t \in [t_k+T, t_{k+1})$.

To conclude the proof, we need to show that the trajectories of the system in any interval $[t_k, t_k+T)$ are bounded and converge to the origin as $k \to \infty$. To do this, let us define the set $\mathcal{S}_\theta = \{\theta = \begin{bmatrix}\theta_f' & \theta_\rho'\end{bmatrix}' \in \mathbb{R}^{2l} : 0 \leq \theta_{fi} \leq 1 \text{ and } 0 \leq \theta_{\rho i} \leq 1,\ i = 1, ..., l\}$, where θ_{fi} and $\theta_{\rho i}$ are the i-th components of θ_f and θ_ρ, respectively. Since (10) and (11) are verified, note that there exists $\theta(t) \in \mathcal{S}_\theta$, such that

$$\begin{aligned} f_i(H_1 x(t)) &= \theta_{fi}(t)\Lambda H_1 x(t) \\ \rho_i(H_2 x(t), H_1 x(t)) &= \theta_{\rho i}(t)\Lambda H_2 x(t) \end{aligned} \qquad \forall i = 1, ..., l$$

Hence, the trajectories of (5) can be represented by the following time-varying linear differential inclusion:

$$\dot{x}(t) = (A_a + B_{af}\Theta_f(t)\Lambda H_1 + B_{a\rho}\Theta_\rho(t)\Lambda H_2)x(t) + B_a \begin{bmatrix} K & 0 \end{bmatrix} x(t_k) \tag{38}$$

with $\Theta_f(t) = \text{diag}(\theta_{f1}(t), ..., \theta_{fl}(t))$ and $\Theta_\rho(t) = \text{diag}(\theta_{\rho 1}(t), ..., \theta_{\rho l}(t))$.

For each admissible function $\theta(t) \in \mathcal{S}_\theta$, since (38) is a linear time-varying system, we can define a transition matrix $\Psi_\theta(t, t_0)$ for it. Defining $\Psi_{\theta_k}(\tau) = \Psi(t_k + \tau, t_k)$ as the restriction of function $\Psi_\theta(t, t_0)$ to the interval $[t_k, t_k + T]$, it follows that

$$\mathcal{X}_k(\tau) = \Psi_{\theta_k}(\tau)\mathcal{X}_k(0) + \int_0^\tau \Psi_{\theta_k}(s)ds B_a \begin{bmatrix} K & 0 \end{bmatrix} \mathcal{X}_k(0)$$

and thus we can write

$$\|\mathcal{X}_k(\tau)\| \leq \left(\left\|\Psi_{\theta_k}(\tau)\right\| + \left\| \int_0^\tau \Psi_{\theta_k}(s)ds \right\| \left\| B_a \begin{bmatrix} K & 0 \end{bmatrix} \right\| \right) \|\mathcal{X}_k(0)\|.$$

Considering all the possible functions $\theta_k \in \mathbb{F}^{2l}_{[0,T]}$ such that $\theta_k(\tau) \in \mathcal{S}_\theta, \forall \tau \in [0, T]$, there exists a scalar

$$\mu_\Psi = \sup_{\theta_k \in \mathbb{F}^{2l}_{[0,T]}, \theta_k(\tau) \in \mathcal{S}_\theta, \tau \in [0\ ,\ T]} \left\{ \left\|\Psi_{\theta_k}(\tau)\right\| + \left\| \int_0^\tau \Psi_{\theta_k}(s)ds \right\| \left\| B_a \begin{bmatrix} K & 0 \end{bmatrix} \right\| \right\}$$

such that $\|\mathcal{X}_k(\tau)\| \leq \mu_\Psi \|\mathcal{X}_k(0)\|$ or, equivalently:

$$\|x(t_k + \tau)\| \leq \mu_\Psi \|x(t_k)\|, \ \forall \tau \in [0, T], \forall k \in \mathbb{N} \tag{39}$$

As (12) and (13) ensure that $V(x(t_k + T)) < V(x(t_k))$ and (14) ensures that $\dot{V}(x(t)) < 0$, $\forall t \in [t_k + T, t_{k+1})$, it follows that $\lim_{k\to\infty} x(t_k) = 0$ and thus from (39), we have that the trajectories are uniformly bounded and $\lim_{t\to\infty} x(t) = 0$.

□

Remark 2. Notice that the proof of Theorem 1 does not require the positive definiteness of the looped-functional $V_0(\tau, \mathcal{X}_k)$. As discussed in [37], this is an advantage (in terms of conservatism reduction) with respect to the use of classical Lyapunov-Krasovskii functionals that are required to be positive definite.

Although the focus in this paper is on event-triggered controllers, as a side effect of the conditions in Theorem 1, the asymptotic stability of the origin of the closed-loop system under periodic sampled control with a period equal to the dwell time T can be formally guaranteed. The following corollary states this.

Corollary 1 (Periodic sampled control)**.** Considering T, K and L given, if there exist symmetric positive definite matrices P and R, a symmetric matrix F_1, matrices $Y_1, Y_2, Y_{1c}, Y_{2c}, F_2, N$ and X and positive definite diagonal matrices S_f, S_ρ, S_{fc} and $S_{\rho c}$ satisfying (12) and (13), then the origin of system (5) is globally asymptotically stable considering a periodic control updating policy, with period T, i.e $t_k = kT$, $\forall k \in \mathbb{N}$.

Proof. It directly follows from Theorem 1. Just notice that for periodic sampling, one needs to consider only the time interval $[t_k, t_k + T]$, therefore condition (14) is not needed. □

6 | CO-DESIGN

In this section, we assume that a stabilizing state feedback control law was previously designed using, for instance, the techniques presented in [42]. From this starting point, the co-design of the observer gain matrix L and the event-triggering function parameters Q_δ and Q_ϵ is addressed.

The following theorem establishes sufficient conditions for the global asymptotic stability of system (5) in the co-design case.

Theorem 2. Considering T and K given, if there exist positive scalars $\epsilon_c, \epsilon_d, \gamma$, symmetric positive definite matrices Q_δ, Q_ϵ, P and R, a non-singular matrix Y_{11}, a symmetric matrix F_1, matrices U, F_2, N and X and positive definite diagonal matrices S_f, S_ρ, S_{fc} and $S_{\rho c}$ satisfying

$$\Pi_1 + T(\Pi_2 + \Pi_3) < 0 \tag{40}$$

$$\begin{bmatrix} \Pi_1 - T\Pi_3 & TN \\ * & -TR \end{bmatrix} < 0 \tag{41}$$

$$\begin{bmatrix} \Pi_a & \Pi_b' \\ * & -Q_\epsilon \end{bmatrix} < 0 \tag{42}$$

with

$$\begin{aligned}
\Pi_1 &= \mathrm{He}\left\{ M_1' P M_3 - N M_{12} - M_{12}' F_2 M_2 \right. \\
&\quad + (\epsilon_d M_1' + M_3') \left[(Y' A_{a1} + L_a) M_1 + Y' B_a \begin{bmatrix} K & 0 \end{bmatrix} M_2 - Y' M_3 + Y' B_{af} M_4 + Y' B_{a\rho} M_5 \right] \\
&\quad \left. - M_4' S_f (M_4 - \Lambda H_1 M_1) - M_5' S_\rho (M_5 + \Lambda H_2 M_1) \right\} - M_{12}' F_1 M_{12}, \\
\Pi_2 &= \mathrm{He}\left\{ M_3' (F_1 M_{12} + F_2 M_2) \right\} + M_3' R M_3, \\
\Pi_3 &= M_2' X M_2, \\
\Pi_a &= \mathrm{He}\left\{ M_1' P M_2 - M_4' S_{fc} (M_4 - \Lambda H_1 M_1) - M_5' S_{\rho c} (M_5 - \Lambda H_2 M_1) \right. \\
&\quad \left. + (\epsilon_c M_1' + M_2') \left[(Y' A_{a1} + L_a + Y' B_a \begin{bmatrix} K & 0 \end{bmatrix}) M_1 - Y' M_2 + Y' B_a K M_3 + Y' B_{af} M_4 + Y' B_{a\rho} M_5 \right] \right\} - M_3' Q_\delta M_3, \\
\Pi_b &= C_a M_1,
\end{aligned}$$

$$A_{a1} = \begin{bmatrix} A_p & 0 \\ 0 & A_p \end{bmatrix}, \; L_a = \begin{bmatrix} 0 & -UC_p \\ 0 & \gamma U C_p \end{bmatrix}, \; Y = \begin{bmatrix} Y_{11} & 0 \\ 0 & \gamma Y_{11} \end{bmatrix},$$

H_1, H_2 and the matrices M_i as defined in (6) and (15), respectively, then the origin of system (5) with $L = (Y_{11}')^{-1} U$ and the triggering rule defined by (8) and (9) is globally asymptotically stable.

Proof. The proof follows the same steps as for Theorem 1. The differences arise from the fact that the conditions in Theorem 1 are not linear if L is a decision variable, due to the terms $2\left(\mathcal{X}'(\tau) Y_1' + \dot{\mathcal{X}}_k'(\tau) Y_2'\right) M_0$ in (22) and $2\left(x'(t) Y_{1c}' + \dot{x}'(t) Y_{2c}'\right) M_{0c}$ in (36). To linearize the conditions, one needs to isolate the terms depending on L in A_a and consider

$$Y_2 = Y_{2c} = Y = \begin{bmatrix} Y_{11} & 0 \\ 0 & \gamma Y_{11} \end{bmatrix}, \; Y_1 = \epsilon_d Y_2, \; Y_{1c} = \epsilon_c Y_{2c},$$

which readily leads to the conditions (40)-(42). □

It should be noticed that the co-design conditions provided by Theorem 2 present additional degrees of freedom, as the observer gain matrix L is a free variable. The co-design approach has therefore the advantage of providing a suitable observer gain matrix that is somewhat optimized for the use in the event-triggered control context. In an emulation context, the designer has no means to take the event-triggering mechanism into account in the design of the observer. Therefore, it is plausible that in many situations co-design will outperform emulation in terms of number of generated events. On the other hand, it should be noticed that to obtain convex conditions, we need to restrict $Y_2 = Y_{2c}$ and also impose a block diagonal structure on these matrices. Due to these constraints, which are not present in the emulation conditions (Theorem 1), in some particular cases, emulation with a particular pre-computed observer can lead to better results.

Remark 3. Theorem 2 provides a condition to co-design only L and the triggering function parameters Q_δ and Q_ϵ. It would be interesting to have K given by the co-design process as well. Unfortunately, from the considered techniques, it was not possible to obtain a convex condition involving the synthesis of K along with L and the triggering function parameters, i.e. expressed in LMI form. It should however be noticed that while there are methods in the literature to design a stabilizing K for the class of the continuous-time systems at hand (see for instance[42]), as the separation principle is not valid for nonlinear systems, there is no systematic methods for designing the observer gain L ensuring the closed-loop stability, even in the continuous-time case. Hence, our co-design condition provides a useful method for that, provided a stabilizing gain K has been previously computed.

7 | OPTIMIZATION PROBLEMS

To compute the triggering function parameters in the emulation context and, additionally, the observer gains in the co-design context, we propose to use the following optimization problems based respectively on the stability conditions of Theorems 1 and 2.

- For the emulation case:

$$\begin{aligned} &\min(\text{tr}(Q_\delta) + \text{tr}(Q_\epsilon)) \\ &\quad \text{subject to: (12), (13), (14), } P > 0 \end{aligned} \tag{43}$$

- For the co-design case:

$$\begin{aligned} &\min(\text{tr}(Q_\delta) + \text{tr}(Q_\epsilon)) \\ &\quad \text{subject to: (40), (41), (42), } P > 0 \end{aligned} \tag{44}$$

The reasoning behind the optimization criterion in (43) and (44) is as follows: According to the triggering rule (8), no events can be generated while $g(\delta(t), y_a(t)) < 0$. Taking the definition of $g(\delta(t), y_a(t))$ from (9), we can rewrite this inequality to conclude that no events can occur while

$$g_1(\delta(t), y_a(t)) = \frac{\delta(t)' Q_\delta \delta(t)}{y_a'(t) Q_\epsilon^{-1} y_a(t)} < 1. \tag{45}$$

Moreover, from the definition of $\delta(t)$ in (7), we see that at each event time we have $\delta(t_k) = 0$. Hence, to trigger a new event, $g_1(\delta(t), y_a(t))$ needs to evolve from 0 to 1. On the other hand, we have

$$g_1(\delta(t), y_a(t)) \leq \frac{\lambda_{max}(Q_\delta)\|\delta\|^2}{\lambda_{min}(Q_\epsilon^{-1})\|y_a\|^2}. \tag{46}$$

The optimization criterion aims at indirectly minimizing the eigenvalues ratio $\frac{\lambda_{max}(Q_\delta)}{\lambda_{min}(Q_\epsilon^{-1})}$ (and thus, maximize the time $g_1(\delta(t), y_a(t))$ takes to go from 0 to 1, maximizing the time between events) by minimizing the sum of the traces of Q_δ and Q_ϵ. Notice that this effectively minimizes the trace of Q_δ and maximizes the trace of Q_ϵ^{-1}, indirectly minimizing the mentioned ratio.

To select the scalars that appear in the co-design case, we propose to use a grid search. The dwell-time parameter T is also a design parameter and can be chosen according to the processing and network communication constraints. The designer can choose, for instance, the smallest dwell time that is suitable given the infrastructure at hand.

8 | NUMERICAL EXAMPLES

In this section, we illustrate the use of the methodology by means of two numerical examples.

8.1 | Example 1

Consider system (1) with:

$$A_p = \begin{bmatrix} 0 & 1 \\ 4 & 0 \end{bmatrix}, \; B_p = \begin{bmatrix} 0 \\ 1 \end{bmatrix}, \; B_{pf} = \begin{bmatrix} 0 \\ 0.5 \end{bmatrix}, \; C_p = \begin{bmatrix} 1 \\ 0 \end{bmatrix}', \; H = \begin{bmatrix} 0 \\ 1 \end{bmatrix}'$$

and $f : \mathbb{R} \to \mathbb{R}$ being a logarithmic function with dead-zone:

$$f(v) = \begin{cases} 0, & \text{if } |v| \leq 1 \\ \ln(v), & \text{if } v > 1 \\ -\ln(-v), & \text{if } v < -1 \end{cases} \tag{47}$$

which leads to $\Lambda = 1$. We choose the controller gain $K = \begin{bmatrix} -6.321 & -3.944 \end{bmatrix}$, which stabilizes the origin of the system in continuous time.

TABLE 1 Example 1 – Average number of control updates for 100 different initial conditions and a simulation of 10 s (emulation case)

T	Event-triggered	Periodic
0.1	18.26	100
0.3	17.54	33
0.4	15.50	25
0.5	unfeasible	20
0.57	unfeasible	unstable

8.1.1 | Emulation

Considering $L = \begin{bmatrix}-4 & -11\end{bmatrix}'$, we solve the emulation optimization problem (43), with additional conditions $\lambda_{max}(Q_\delta) < 10^3\lambda_{min}(Q_\delta)$ and $\lambda_{max}(Q_\epsilon) < 10^3\lambda_{min}(Q_\epsilon)$ to prevent Q_δ and Q_ϵ from becoming ill-conditioned, for $T = 0.1$, $T = 0.3$ and $T = 0.4$. Simulations of the resulting closed-loop systems for these cases, considering the initial condition $x_p(0) = \begin{bmatrix}-4 & -3\end{bmatrix}'$, $\hat{x}(0) = \begin{bmatrix}0 & 0\end{bmatrix}'$ are depicted in Figure 1. The upper plots in the figure depict the states of the plant and of the observer. One can see that the states of the closed-loop systems indeed converge to the origin. The middle plots depict the control signal. The bottom plots depict the instants where the events occurred. The heights of the bars in the bottom plot represent the inter-event times $t_k - t_{k-1}$ and the horizontal line represents the dwell time T. The numbers of events in these plots are 20, 19 and 16, respectively. One can see that the event-triggering mechanism effectively postpones the occurrence of events with respect to the dwell time (i.e. there is an improvement with respect to a periodic implementation with period T). To confirm this improvement, we calculated the average number of samples for simulations of the closed-loop systems considering 100 initial conditions along the unit circle on the plane containing the plant state variables, i.e., considering various initial conditions of the plant and zero-initialized observers, and the time interval [0, 10]. The results are summarized in Table 1, which also shows the number of events generated by a periodic implementation with a sampling period equal to the dwell time T.

For $T = 0.5$, the optimization problem becomes unfeasible. A periodic implementation of the controller with a sampling period of 0.5 is still stable, but it would be outperformed by any of the event-triggered control implementations considering dwell times less than or equal to 0.4, as shown in Table 1. Periodic implementations with sampling periods of 0.57 and above are unstable, as shown in Figure 2. Therefore, the event-triggered control implementation with $T = 0.4$ outperforms any periodic implementation for the example at hand.

8.1.2 | Co-design

Considering the dwell times $T = 0.1$, $T = 0.3$ and $T = 0.4$, we solve the co-design optimization problem (44) with additional conditions $\lambda_{max}(Q_\delta) < 10^3\lambda_{min}(Q_\delta)$ and $\lambda_{max}(Q_\epsilon) < 10^3\lambda_{min}(Q_\epsilon)$ to prevent Q_δ and Q_ϵ from becoming ill-conditioned. Simulations of the resulting closed-loop systems considering the initial condition $x_p(0) = \begin{bmatrix}-4 & -3\end{bmatrix}'$, $\hat{x}(0) = \begin{bmatrix}0 & 0\end{bmatrix}'$ are depicted in Figure 3. The numbers of events generated were 18, 17 and 15. As in the emulation case, Table 2 shows the average number of events obtained for each value of the dwell time, considering the time interval [0, 10] and 100 initial conditions distributed along the unit circle in the plane of the plant states with zero-initialized observers. The number of events generated by a periodic implementation with a sampling period equal to the dwell time T is also shown for comparison. As in the emulation case, the event-triggering mechanism effectively postponed the occurrence of events with respect to the dwell time, representing an improvement with respect to a periodic implementation with period T.

For $T = 0.5$, the optimization problem becomes unfeasible. In this case, it makes no sense to compare to a periodic implementation since the observer gain matrix L is not defined when the optimization problem is unfeasible.

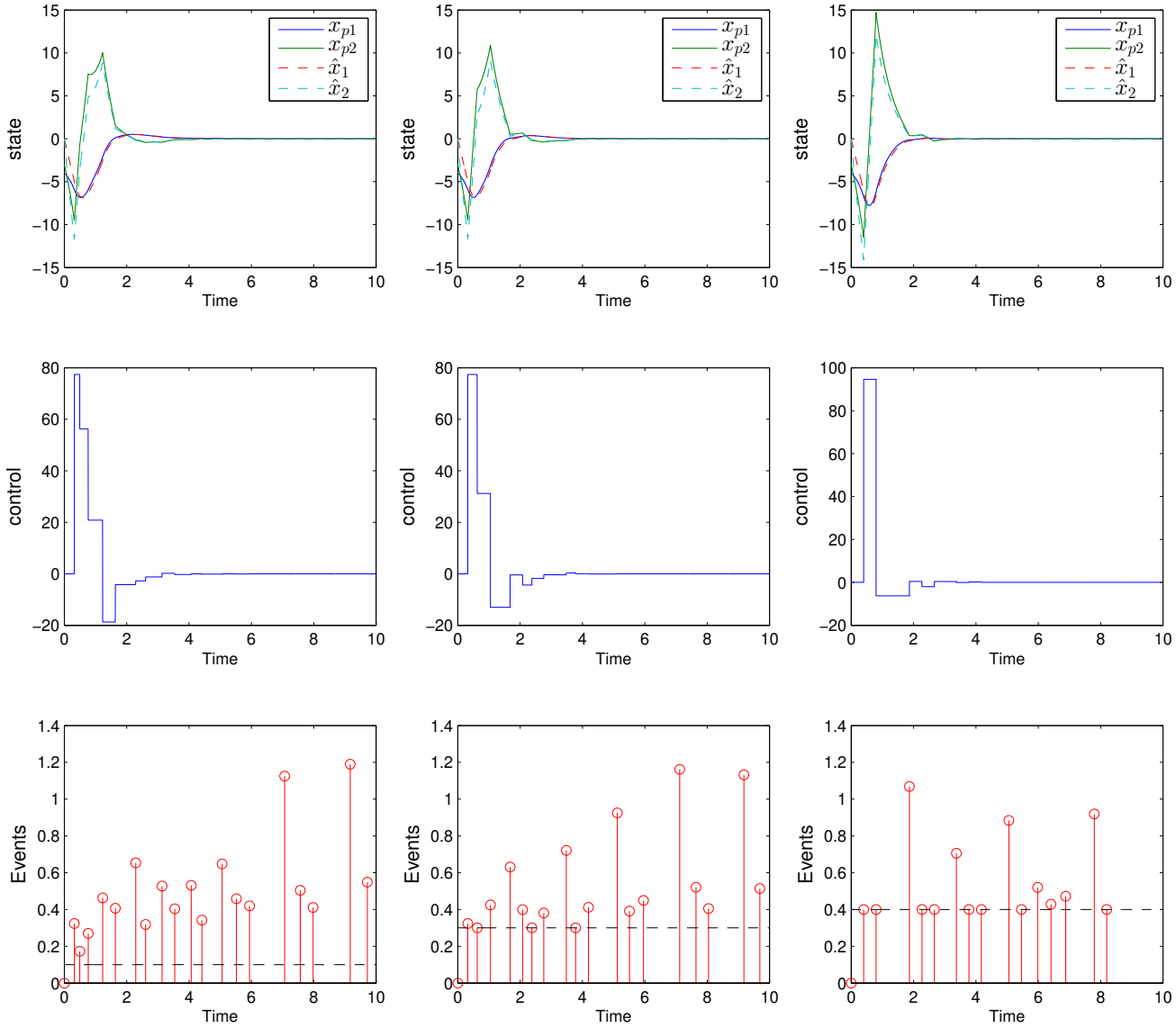

a) $T = 0.1$ b) $T = 0.3$ c) $T = 0.4$

FIGURE 1 Example 1 – Emulation design – Simulations for some values of T.

8.2 | Example 2

In this section we consider a one-link robotic manipulator with flexible joints driven by a DC motor, as presented in[43] and[44]. The system admits a representation as given in (1) with:

$$A_p = \begin{bmatrix} 0 & 1 & 0 & 0 \\ -48.6 & -1.25 & 48.6 & 0 \\ 0 & 0 & 0 & 1 \\ 19.5 & 0 & -16.7 & 0 \end{bmatrix}, \; B_p = \begin{bmatrix} 0 \\ 21.6 \\ 0 \\ 0 \end{bmatrix}, \; B_{pf} = \begin{bmatrix} 0 \\ 0 \\ 0 \\ -3.33 \end{bmatrix}, \; C_p' = \begin{bmatrix} 1 & 0 \\ 0 & 1 \\ 0 & 0 \\ 0 & 0 \end{bmatrix}, \; H' = \begin{bmatrix} 0 \\ 0 \\ 1 \\ 0 \end{bmatrix}$$

with $f : \mathbb{R} \to \mathbb{R}$ defined as

$$f(v) = \sin(v) + v \tag{48}$$

It follows that $f(v)$ satisfies assumptions (A1) and (A2) with $\lambda = 2$.

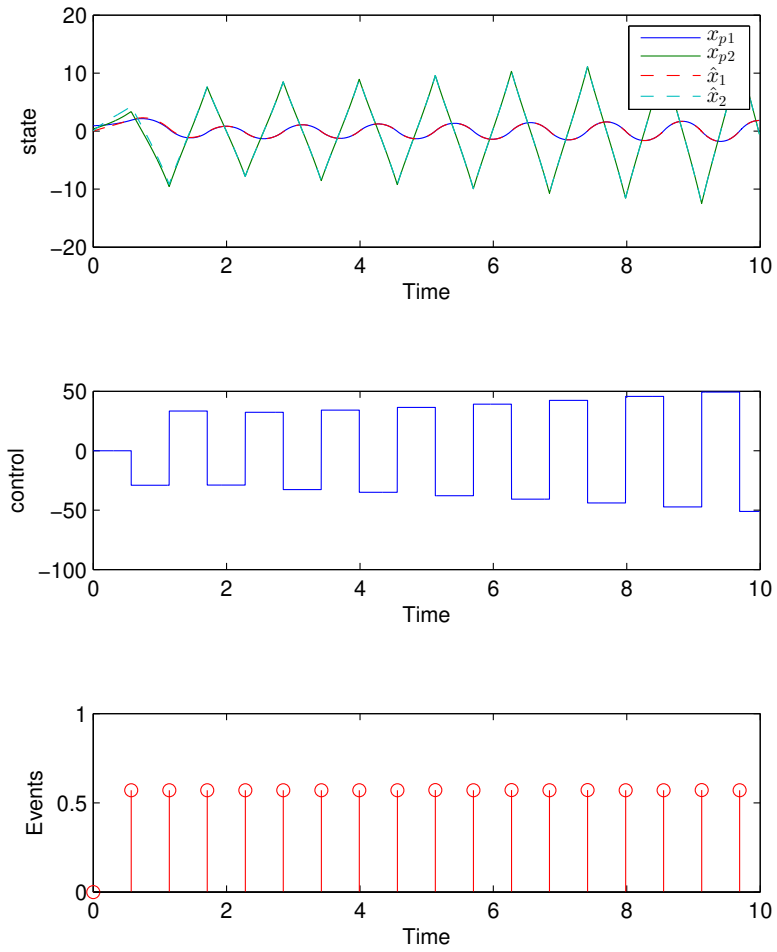

FIGURE 2 Example 1 – Periodic implementation with sampling period of 0.57.

TABLE 2 Example 1 – Average number of control updates for 100 different initial conditions and a simulation of 10 s (co-design case)

T	Event-triggered	Periodic
0.1	16.36	100
0.3	18.08	33
0.4	14.18	25
0.5	unfeasible	–

In this representation, x_1 and x_2 are the motor axis angular position and velocity, respectively, while x_3 and x_4 are the arm angular position and velocity. As in[44], we assume that only the motor axis variables are measurable and that we are interested in steering the state to zero. We are specifically interested in the arm variables x_3 and x_4.

For the controller, we choose the gain $K = \begin{bmatrix} -9.044 & -1.385 & 3.810 & -1.140 \end{bmatrix}$, which globally stabilizes the origin of the system in continuous time.

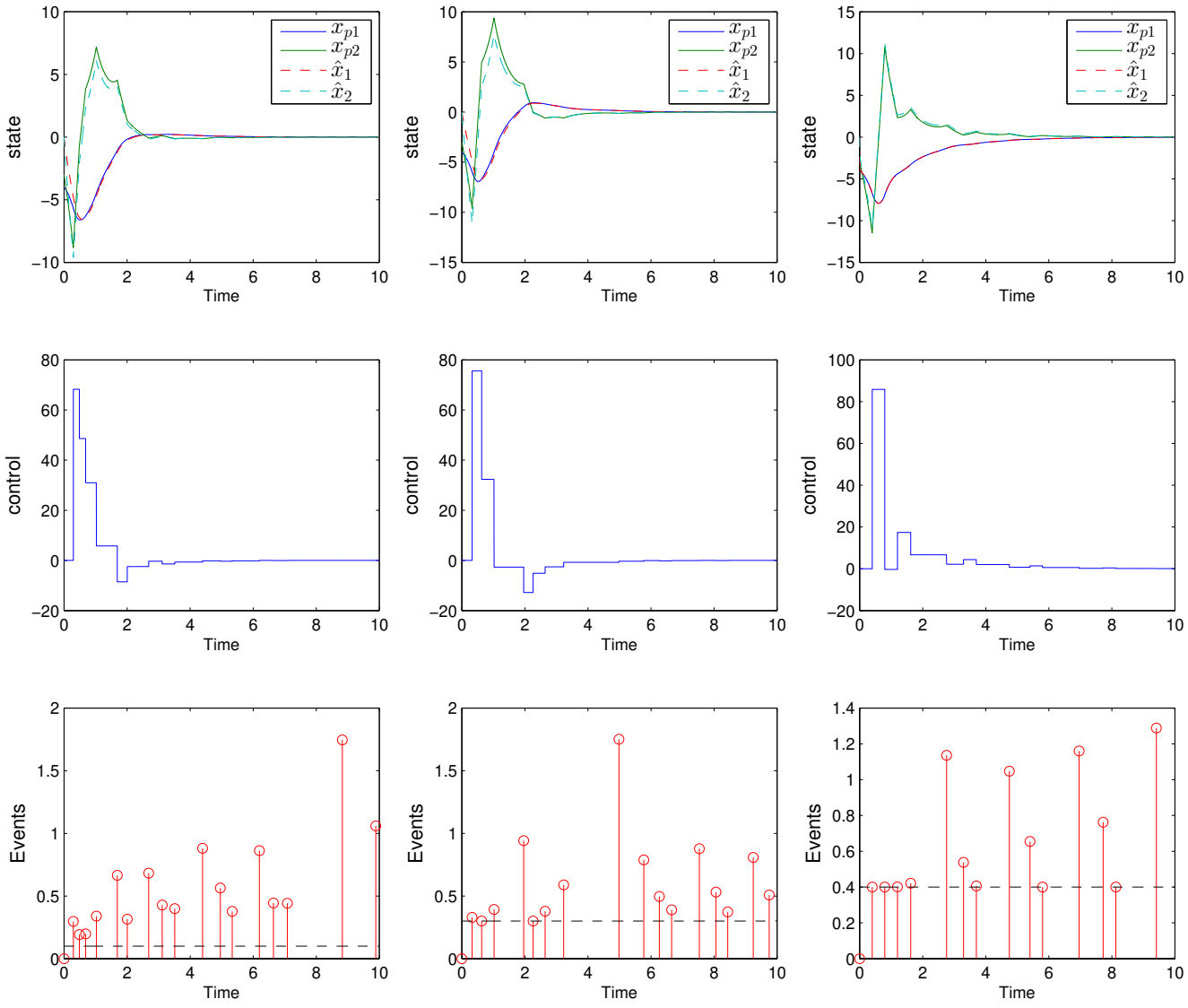

a) $T = 0.1$ b) $T = 0.3$ c) $T = 0.4$

FIGURE 3 Example 1 – Co-design – Simulations for some values of T.

8.2.1 | Emulation

Considering

$$L = \begin{bmatrix} -3.221 & -18.78 & -1.724 & 2.835 \\ 0.2411 & -39.72 & -0.4128 & 0.4373 \end{bmatrix},$$

we solve optimization problem (43), with additional conditions $\lambda_{max}(Q_\delta) < 10^3 \lambda_{min}(Q_\delta)$ and $\lambda_{max}(Q_\epsilon) < 10^3 \lambda_{min}(Q_\epsilon)$ to prevent Q_δ and Q_ϵ from becoming ill-conditioned, for $T = 0.02$ and $T = 0.04$. Simulations of the resulting closed-loop systems for these cases, considering the initial conditions $x_p(0) = \begin{bmatrix} 1.2 & 0 & 0 & 0 \end{bmatrix}'$, borrowed from[43], and $\hat{x}(0) = \begin{bmatrix} 0 & 0 & 0 & 0 \end{bmatrix}'$ are depicted in Figure 4. The upper plots in the figure depict the angular position and velocity of the arm, in solid lines, as well as the corresponding observed state variables, in dashed lines. One can see that the state variables indeed converge to the origin. The numbers of events in these plots are 80 and 72, respectively. It can be seen again that the event-triggering mechanism effectively postpones the occurrence of events with respect to the dwell time.

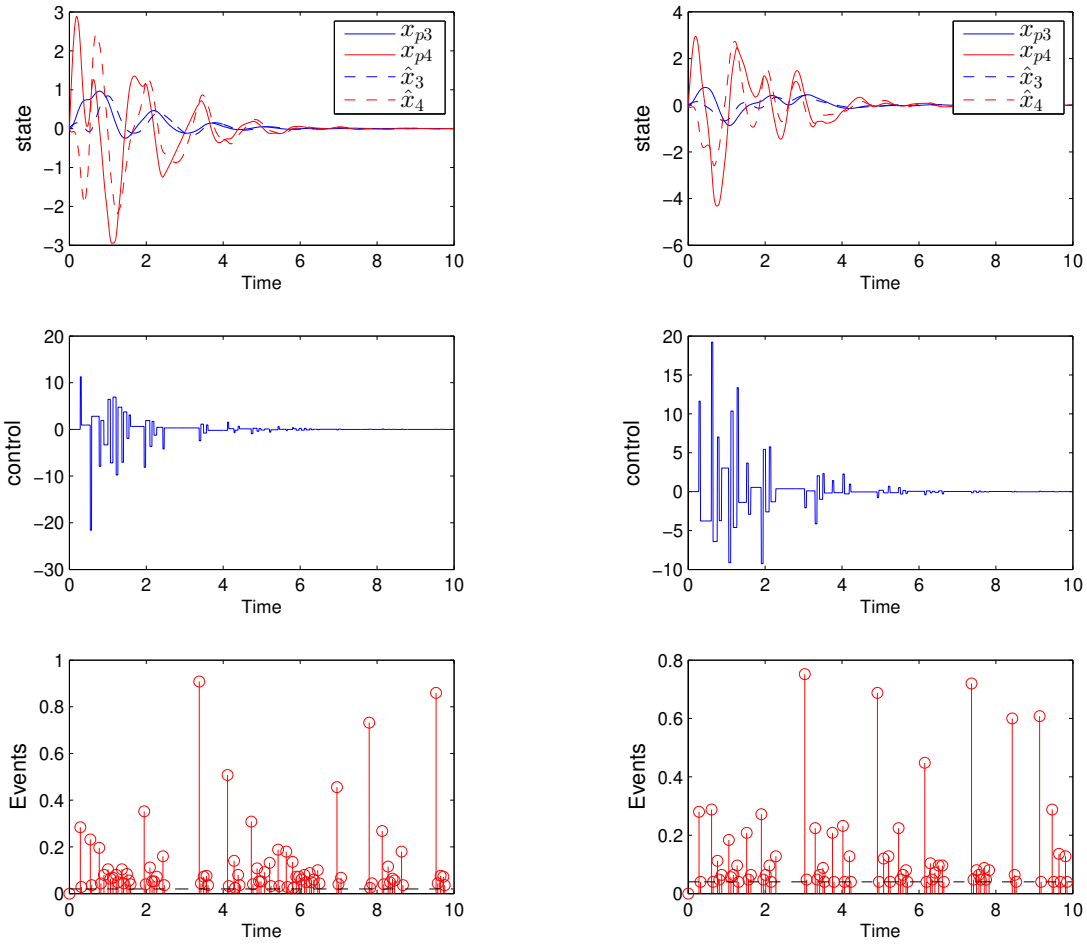

a) $T = 0.02$ b) $T = 0.04$

FIGURE 4 Example 2 – Emulation design – Simulations for some values of T.

8.2.2 | Co-design

Considering the dwell times $T = 0.02$ and $T = 0.04$, we solve the co-design optimization problem (44), also with the additional conditions $\lambda_{max}(Q_\delta) < 10^3\lambda_{min}(Q_\delta)$ and $\lambda_{max}(Q_\epsilon) < 10^3\lambda_{min}(Q_\epsilon)$ to prevent Q_δ and Q_ϵ from becoming ill-conditioned. Simulations of the resulting closed-loop systems with the same initial conditions $x_p(0) = \begin{bmatrix}1.2 & 0 & 0 & 0\end{bmatrix}'$ and $\hat{x}(0) = \begin{bmatrix}0 & 0 & 0 & 0\end{bmatrix}'$ are depicted in Figure 5. The number of events are 81 and 55, respectively. As one can see, the event-triggering strategy resulting from the co-design process also effectively postponed the occurrence of events with respect to the dwell time in this example.

9 | CONCLUSION

In this paper we addressed the design of observer-based event-triggered control for systems with slope-restricted nonlinearities that depend on the system state. Emulation design as well as the co-design of the triggering function parameters and the observer gain matrix have been addressed. From a practical perspective, the proposed approach is based only on available information: the control strategy depends only on the measurable output of the plant and the triggering rule depends only on this measure and the observer states. In particular, as the nonlinearity of the system is supposed to be non-measurable, the proposed observer contains a nonlinearity that depends only on the estimated state. The mismatch between the nonlinearities of the system and the observer leads to a nonlinear behavior for the observation error. To tackle this issue, a "sector-like" relation is considered for the mismatched term. Thus, sufficient conditions in the form of LMIs associated to convex optimization problems have

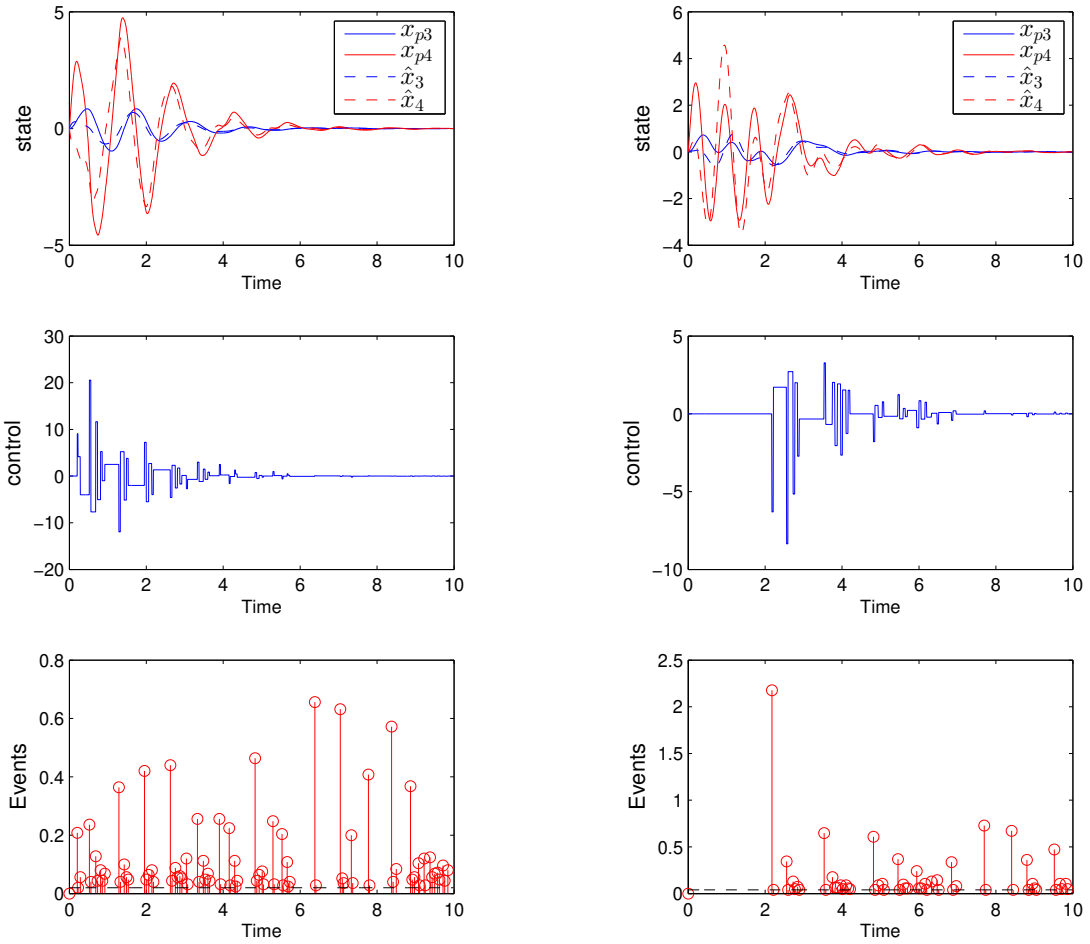

a) $T = 0.02$ b) $T = 0.04$

FIGURE 5 Example 2 – Co-design – Simulations for some values of T.

been proposed to design the triggering function parameters and the observer gains (in the co-design case) to ensure the global asymptotic stability of the closed-loop system while aiming at reducing the number of events. The approach allows to design the event-triggering strategy with a dwell time T imposing a minimum inter-events time, which prevents the Zeno behavior occurrence. To ensure asymptotic stability in the presence of this dwell time, a looped-functional approach was considered. This approach ensures that the trajectories remain bounded during the dwell time and that the total variation of a quadratic Lyapunov function over this time is negative. The looped-functional approach also permits to derive conditions that ensure the asymptotic stability of a periodic sampled implementation of the controller, which was presented as a corollary to the main result. Two numerical examples illustrated the effectiveness and potential of the proposed methods in reducing the number of control updates.

The simultaneous design of the event-triggering strategy, the observer and the control gains is still an open problem and subject of ongoing work. Future work directions also include extending the proposed design method to take into consideration usual network-induced constraints such as time delays, packet losses and loss of packet ordering.

ACKNOWLEDGMENTS

This work was supported in part by CAPES (PhD Scholarship of L. G. Moreira, PDSE 88881.134305/2016-01 and Proj. STICAmSud 88881.143275/2017-01), by CNPQ (grants PQ-307449/2019-0 and Univ-422992/2016-0), by IFSUL (Project PD00190519/011), Brazil and by ANR via project HANDY number ANR-18-CE40-0010, France.

References

1. Postoyan R, Girard A. Triggering mechanism using freely selected sensors for linear time-invariant systems. In: Proceedings of the IEEE Conference on Decision and Control. IEEE; 2015; Osaka, Japan: 4812-4817.

2. Postoyan R, Tabuada P, Nešić D, Anta A. A framework for the event-triggered stabilization of nonlinear systems. *IEEE Trans. Autom. Control* 2015; 60(4): 982-996.

3. Tabuada P. Event-triggered real-time scheduling of stabilizing control tasks. *IEEE Trans. Autom. Control* 2007; 52(9): 1680-1685.

4. Heemels WPMH, Johansson KH, Tabuada P. An introduction to event-triggered and self-triggered control. In: Proceedings of the IEEE Conference on Decision and Control. IEEE; 2012; Maui: 3270-3285.

5. Selivanov A, Fridman E. Event-Triggered H_∞ Control: A Switching Approach. *IEEE Trans. Autom. Control* 2016; 61(10): 3221-3226.

6. Selivanov A, Fridman E. Observer-based input-to-state stabilization of networked control systems with large uncertain delays. *Automatica* 2016; 74: 63-70.

7. Borgers DP, Dolk VS, Heemels WPMH. Riccati-Based Design of Event-Triggered Controllers for Linear Systems With Delays. *IEEE Trans. Autom. Control* 2018; 63(1): 174-188.

8. Abdelrahim M, Dolk VS, Heemels WPMH. Event-triggered quantized control for input-to-state stabilization of linear systems with distributed output sensors. *IEEE Trans. Autom. Control* 2019: 1-16.

9. Wang X, Lemmon MD. Event design in event-triggered feedback control systems. In: Proceedings of the IEEE Conference on Decision and Control. IEEE; 2008; Cancun, Mexico: 2105-2110.

10. Abdelrahim M, Postoyan R, Daafouz J, Nešić D. Stabilization of nonlinear systems using event-triggered output feedback controllers. *IEEE Trans. Autom. Control* 2016; 61(9): 2682-2687.

11. Jiang B, Karimi HR, Kao Y, Gao C. Takagi–Sugeno Model Based Event-Triggered Fuzzy Sliding-Mode Control of Networked Control Systems With Semi-Markovian Switchings. *IEEE Transactions on Fuzzy Systems* 2020; 28(4): 673-683.

12. Antunes D, Heemels WPMH, Tabuada P. Dynamic programming formulation of periodic event-triggered control: Performance guarantees and co-design. In: Proceedings of the IEEE Conference on Decision and Control. IEEE; 2012; Maui, USA: 7212–7217.

13. Heemels WPMH, Donkers MCF, Teel AR. Periodic event-triggered control for linear systems. *IEEE Trans. Autom. Control* 2013; 58(4): 847–861.

14. Abdelrahim M, Postoyan R, Daafouz J, Nešić D. Co-design of output feedback laws and event-triggering conditions for linear systems. In: Proceedings of the IEEE Conference on Decision and Control. IEEE; 2014; Los Angeles: 3560-3565.

15. Abdelrahim M, Postoyan R, Daafouz J, Nešić D, Heemels WPMH. Co-design of output feedback laws and event-triggering conditions for the $\mathcal{L}_2$-stabilization of linear systems. *Automatica* 2018; 87: 337 - 344.

16. Seuret A, Prieur C, Tarbouriech S, Zaccarian L. Event-triggered sampling for linear closed-loop systems with plant input saturation. In: Proceedings of the IFAC Symposium on Nonlinear Control Systems. Elsevier; 2013; Toulouse, France: 341-346.

17. Seuret A, Prieur C, Tarbouriech S, Zaccarian L. LQ-based event-triggered controller co-design for saturated linear systems. *Automatica* 2016; 74: 47-54.

18. Wang Y, Lei Y, Bian T, Guan Z. Distributed Control of Nonlinear Multiagent Systems With Unknown and Nonidentical Control Directions via Event-Triggered Communication. *IEEE Transactions on Cybernetics* 2019; online: 1-13.

19. Lei Y, Wang Y, Guan Z, Shen Y. Event-Triggered Adaptive Output Regulation for a Class of Nonlinear Systems With Unknown Control Direction. *IEEE Transactions on Systems, Man, and Cybernetics: Systems* 2018; online: 1-8.

20. Wang D, Ha M, Qiao J. Self-Learning Optimal Regulation for Discrete-Time Nonlinear Systems Under Event-Driven Formulation. *IEEE Transactions on Automatic Control* 2020; 65(3): 1272-1279.

21. Wang D, Liu D. Learning and Guaranteed Cost Control With Event-Based Adaptive Critic Implementation. *IEEE Transactions on Neural Networks and Learning Systems* 2018; 29(12): 6004-6014.

22. Lehmann D, Lunze J. Extension and experimental evaluation of an event-based state-feedback approach. *Control Engineering Practice* 2011; 19(2): 101-112.

23. Wu W, Reimann S, Liu S. Event-triggered control for linear systems subject to actuator saturation. *IFAC Proceedings Volumes* 2014; 47(3): 9492-9497. 19th IFAC World Congress.

24. Aranda-Escolastico E, Guinaldo M, Dormido S. A novel approach for periodic event-triggering based on general quadratic functions. In: Proceedings of the International Conference on Event-based Control, Communication, and Signal Processing. IEEE; 2015; Krakow: 1-6.

25. Moreira LG, Groff LB, Gomes da Silva Jr. JM. Event-triggered state-feedback control for continuous-time plants subject to input saturation. *Journal of Control, Automation and Electrical Systems* 2016; 27(5): 473-484.

26. Moreira LG, Groff LB, Gomes da Silva Jr. JM, Coutinho D. Event-triggered control for nonlinear rational systems. *IFAC-PapersOnLine* 2017a; 50(1): 15307-15312. 20th IFAC World Congress.

27. Goebel R, Sanfelice RG, Teel AR. *Hybrid dynamical systems: modeling, stability, and robustness*. New York: Princeton University Press . 2012.

28. Dolk VS, Borgers DP, Heemels WPMH. Output-Based and Decentralized Dynamic Event-Triggered Control With Guaranteed $\mathcal{L}_p$- Gain Performance and Zeno-Freeness. *IEEE Trans. Autom. Control* 2017; 62(1): 34-49.

29. Yu H, Antsaklis PJ. Event-triggered output feedback control for networked control systems using passivity: Achieving $\mathscr{L}_2$ stability in the presence of communication delays and signal quantization. *Automatica* 2013; 49(1): 30 - 38.

30. Xia C, Fei H. Observer based event-triggered control for certain and uncertain linear systems. *IMA Journal of Mathematics Control and Information* 2013; 30(4): 1-16.

31. Feng J, Li N. Design of observer-based event-driven controllers for a class of state-dependent nonlinear systems. *Journal of the Franklin Institute* 2016; 353(7): 1573 - 1593.

32. Xing L, Wen C, Liu Z, Su H, Cai J. Event-Triggered Output Feedback Control for a Class of Uncertain Nonlinear Systems. *IEEE Trans. Autom. Control* 2019; 64(1): 290-297.

33. Moreira LG, Tarbouriech S, Seuret A, Gomes da Silva Jr. JM. Observer-based event-triggered control in the presence of cone-bounded nonlinear inputs. *Nonlinear Analysis: Hybrid Systems* 2019; 33: 17 - 32.

34. Matsumoto T. A chaotic attractor from Chua's circuit. *IEEE Transactions on Circuits and Systems* 1984; 31(12): 1055-1058.

35. Mazo M, Anta A, Tabuada P. An ISS self-triggered implementation of linear controllers. *Automatica* 2010; 46(8): 1310-1314.

36. Seuret A, Gomes da Silva Jr. JM. Taking into account period variations and actuators saturation in sampled-data systems. *Systems & Control Letters* 2012; 61(12): 1286-1293.

37. Seuret A. A novel stability analysis of linear systems under asynchronous samplings. *Automatica* 2012; 48(1): 177 - 182.

38. Briat C, Seuret A. A looped-functional approach for robust stability analysis of linear impulsive systems. *Systems & Control Letters* 2012; 61(10): 980-988.

39. Gomes da Silva Jr. J, Castelan E, Corso J, Eckhard D. Dynamic output feedback stabilization for systems with sector-bounded nonlinearities and saturating actuators. *Journal of the Franklin Institute* 2013; 350(3): 464 - 484.

40. Yamamoto Y. New approach to sampled-data control systems - a function space method. In: Proceedings of the IEEE Conference on Decision and Control. IEEE; 1990; Honolulu: 1882-1887.

41. Briat C. Convergence and Equivalence Results for the Jensen's Inequality – Application to Time-Delay and Sampled-Data Systems. *IEEE Trans. Autom. Control* 2011; 56(7): 1660-1665.

42. Castelan EB, Tarbouriech S, Queinnec I. Control design for a class of nonlinear continuous-time systems. *Automatica* 2008; 44(8): 2034-2039.

43. Böhm C, Yu S, Findeisen R, Allgöwer F. Predictive control for lure systems subject to constraints using LMIs. In: ; 2009: 3389-3394.

44. Rajamani R, Cho YM. Existence and design of observers for nonlinear systems: Relation to distance to unobservability. *International Journal of Control* 1998; 69(5): 717-731.